Exploratory analysis of serum concentrations of oocyte biomarkers growth differentiation factor 9 and bone morphogenetic protein 15 in ovulatory women across the menstrual cycle

Angelique H. Riepsamen, Ph.D.,[a] Mark W. Donoghoe, Ph.D.,[b] Angela Baerwald, M.D., Ph.D.,[c,d] Michael W. Pankhurst, Ph.D.,[e] Shelly Lien, B.Sc.,[a] Yih Harng Chong, Ph.D.,[e] David M. Robertson, Ph.D.,[a] William L. Ledger, M.D., Ph.D.,[a] and Robert B. Gilchrist, D.Sc.[a]

[a] Fertility and Research Centre, School of Women's and Children's Health, and [b] Stats Central, Mark Wainwright Analytical Centre, University of New South Wales Sydney, New South Wales, Australia; [c] Department of Academic Family Medicine, West Winds Primary Health Center, Saskatchewan, Canada; [d] College of Medicine, University of Saskatchewan, Saskatoon, Saskatchewan, Canada; and [e] Department of Anatomy, School of Biomedical Sciences, University of Otago, Dunedin, New Zealand

Objective: To characterize and evaluate the variation in serum concentrations of oocyte-secreted growth differentiation factor 9 (GDF9) and bone morphogenetic protein 15 (BMP15) throughout the menstrual cycle in women from young to advanced reproductive ages.
Design: Cross-sectional, observational, and exploratory study.
Setting: Multicenter university-based clinical practices and laboratories.
Patient(s): Serum was collected every 1–3 days throughout the menstrual cycle from 3 cohorts of healthy, ovulatory women: menses to late luteal phase (21–29 years of age; n = 16; University of Otago) and across one interovulatory interval (18-35 years of age; n = 10; and 45–50 years of age; n = 15; University of Saskatchewan).
Intervention(s): None.
Main Outcome Measure(s): To detect the changes in serum GDF9 and BMP15 across the cycle, mean concentration and variance were statistically modeled using a generalized additive model of location, shape and scale (GAMLSS). Follicle-stimulating hormone, luteinizing hormone, estradiol, progesterone, and anti-Müllerian hormone were also assessed.
Result(s): GDF9 and BMP15 were detectable in 54% and 73% of women and varied 236-fold and 52-fold between women, respectively. Across the menstrual cycle, there were minimal changes in GDF9 or BMP15 within a woman for all cohorts, with no significant differences detected in the modeled mean concentrations. However, modeled variances were highest in the luteal phases of all women for BMP15 immediately after ovulation, regardless of age.
Conclusion(s): Serial changes in GDF9 or BMP15 concentrations across the cycle were not statistically detected and are likewise similar across the reproductive lifespan. Further research is required to fully elucidate the utility of these oocyte biomarkers at diagnosing fertility potential and/or disease. (Fertil Steril® 2021;■:■–■. ©2021 by American Society for Reproductive Medicine.)
Key Words: Oocyte-secreted factors, biomarker, anti-Müllerian hormone (AMH), follicular phase, luteal phase

Discuss: You can discuss this article with its authors and other readers at https://www.fertstertdialog.com/posts/31462

Received September 20, 2020; revised January 18, 2021; accepted February 1, 2021.
A.H.R. reports Patent WO2018/141015A1 under consideration, director and shareholder for Anlagen Pty Ltd for the submitted work. D.M.R. reports grant from National Health & Medical Research Council, Patent WO2018/141015A1 under consideration, director and shareholder for Anlagen Pty Ltd for the submitted work. M.W.D. has nothing to disclose. A.B. has nothing to disclose. M.W.P. has nothing to disclose. S.L. has nothing to disclose. Y.H.C. has nothing to disclose. W.L.L. reports grants from National Health & Medical Research Council and City Fertility Centre Global Pty Ltd, Patent WO2018/141015A1 under consideration, director and shareholder for Anlagen Pty Ltd for the submitted work. R.B.G. reports grants from National Health & Medical Research Council and City Fertility Centre Global Pty Ltd, Patent WO2018/141015A1 under consideration, director and shareholder for Anlagen Pty Ltd for the submitted work.
Reprint requests: Angelique H. Riepsamen, Ph.D., Rm 447, Wallace Wurth Bldg C27, UNSW Sydney, NSW 2052, Australia (E-mail: a.riepsamen@unsw.edu.au).

Fertility and Sterility® Vol. ■, No. ■, ■ 2021 0015-0282/$36.00

https://doi.org/10.1016/j.fertnstert.2021.02.001

The menstrual cycle in healthy, ovulatory women of reproductive age is characterized by changes in the pituitary and reproductive hormones, responsible for regulating folliculogenesis, ovulation, corpus luteum formation, and ovarian reserve (1, 2). Serum concentrations of pituitary-derived hormones, follicle-stimulating hormone (FSH) and luteinizing hormone (LH), and ovarian hormones, estradiol, progesterone, inhibin A, and inhibin B, are used to clinically predict stages of the menstrual cycle, assess female fertility, and guide the treatment of reproductive disorders. Dynamic hormonal interactions are altered as a woman approaches the late reproductive phase. As the growing pool of oocytes declines with age, pituitary FSH and LH increase because of a reduction in the negative feedback factors (primarily inhibin B and estradiol) produced by the ovarian follicular granulosa cells (3–6). Further, serum concentrations of anti-Müllerian hormone (AMH, a protein within the transforming growth factor-β superfamily), produced by the granulosa cells from preantral and antral follicles, also decline (5–7). AMH is considered a useful indirect biomarker of the ovarian reserve because it dramatically declines with age, in parallel with the decline in antral follicle count (AFC). Small changes in serum AMH across the menstrual cycle have been identified after multiple sampling, with the highest levels observed during the midfollicular phase, decreasing at approximately the time of ovulation (8); however, the overall changes across the cycle appear limited and, at present, do not detract from its clinical application as a marker of AFC. Nonetheless, AMH as well as inhibin B and estradiol, are produced by granulosa cells and do not provide an assessment of oocyte quality. Currently, there is no clinically available serum biomarker of the oocyte itself for assessment of oocyte developmental potential or ovarian reserve. If an oocyte-secreted product could be measured reliably in serum it could prove valuable as a biomarker of ovarian reserve, ovarian disease, and/or oocyte quality.

Growth differentiation factor 9 (GDF9) and bone morphogenetic protein 15 (BMP15) are 2 proteins of the transforming growth factor-β superfamily that are predominantly produced by the oocyte (9). These oocyte-secreted factors have pivotal roles in regulating mammalian folliculogenesis and fecundity (10–12). These characteristics make GDF9 and BMP15 ideal candidates as potential diagnostic biomarkers of oocyte function. They are paracrine growth factors that regulate early follicular growth and development, granulosa cell proliferation, and prevention of luteinization, and they determine cumulus cell lineage differentiation and function before ovulation (10, 12–14). GDF9 and BMP15 act as homodimers, and likely as heterodimers, to elicit these effects; however, their primary bioactive forms in vivo are unknown (15, 16). In humans, GDF9 and BMP15 mRNA are expressed throughout nearly all stages of folliculogenesis. GDF9 is highly expressed in oocytes from primordial, primary, secondary, antral, and preovulatory follicles, and in MII oocytes. By comparison, BMP15 expression is observed in oocytes of follicles $\geq$75 μm, increasing in expression throughout folliculogenesis, and highest in oocytes from antral and preovulatory follicles, and in MII oocytes (17–23). In humans, mutations in these oocyte-secreted factors have been linked to ovulation defects, premature ovarian insufficiency, twinning, and subfertility ([24–27], as reviewed by Persani et al. [13]). Although mRNA expression profiles have been characterized throughout folliculogenesis, protein levels of GDF9 and BMP15 in oocytes or biological fluids are less well-characterized, principally due to assay limitations to date. For example, it is unknown if oocyte expression or secretion of these proteins changes throughout the menstrual cycle in women or if they are affected by changes in the ovarian-pituitary axis that accompany reproductive aging. We postulated that the levels of GDF9 and BMP15 may vary within a subject across the menstrual cycle, as these growth factors are critically important for cumulus expansion and ovulation (reviewed by Richani and Gilchrist [28] and Russell et al. [29]), and there are periovulatory changes in BMP15 mRNA and protein levels in rodents (30–32).

Despite being intrafollicular paracrine growth factors, low concentrations (pg/mL) of GDF9 and BMP15 have been detected in the serum of women. Analysis of concentrations of GDF9 and BMP15 relative to other reproductive hormones measured on day 2 of menses found no correlation with AMH or FSH (33). However, GDF9 and BMP15 have not been assessed in healthy, ovulatory women across the menstrual cycle, or in relation to other reproductive hormones, such as LH, estradiol, and progesterone. This study aimed to determine whether serum GDF9 and BMP15 vary across the menstrual cycle in healthy, ovulatory women of reproductive and advanced reproductive age, as a first step toward assessing whether these oocyte-secreted growth factors could be useful biomarkers of ovarian function and/or oocyte quality.

MATERIAL AND METHODS

Study Participants

Healthy, ovulatory women of reproductive age with a history of regular menstrual cycles were recruited as part of 2 independent, prospective, cross-sectional studies at the University of Saskatchewan, Canada, and the University of Otago, New Zealand, as described previously (6, 34). Studies were approved by the Biomedical Research Ethics Board at the University of Saskatchewan and the Strategic Priorities Planning Committee of the Saskatoon Health Region, and the University of Otago Human Ethics Committee (Health), respectively. Exclusion criteria included pregnancy, lactation, medical conditions, or use of medications known or suspected to interfere with reproductive or endocrine function (including hormonal contraceptives) for at least 3 months before study participation, and body mass index (BMI) $<$18 or $>$35 kg/m^2. From these previously recruited women, 3 cohorts of women were selected to examine the serum GDF9 and BMP15: early reproductive age (ERA) – Otago, 21–29 years (n = 16); mid reproductive age (MRA) – Saskatchewan, 18–35 years (n = 10); and advanced reproductive age (ARA) – Saskatchewan, 45–50 years (n = 15; Table 1). Eligible women aged 18–44 years (ERA and MRA cohorts) had a history of regular menstrual cycles (21–35 days), and women 45–50 years (ARA cohort) were eligible

TABLE 1

Participant demographics, cycle characteristics, and mean/baseline endocrine concentrations between cohorts.

	ERA	MRA	ARA	*P* value	Post-hoc
Origin	Otago, New Zealand	Saskatchewan, Canada	Saskatchewan, Canada		
No. of participants	16	10	15		
Demographics					
Age range, y (mean ± SD)	21–29 (24.8 ± 2.3)	18–35 (27.0 ± 6.2)	45–50 (48.0 ± 1.9)	<.0001*	ERA vs. ARA *P*<.0001 MRA vs. ARA *P*<.0001
BMI, kg/m^2 (mean ± SD)	24.7 ± 2.8	27.5 ± 4.0	26.0 ± 3.6	.157	
Cycle characteristics					
Cycle length/IOI, days median, (range) Mean ± SD	30 (26–33) 29.3 ± 2.3	27.5 (23–35) 28.0 ± 3.4	26 (17–41) 26.9 ± 5.2	.044*	ERA vs. ARA *P*<.05
AFC					
>6 mm, mean ± SD	N/Aˆ	8.00 ± 3.74	2.50 ± 1.17	<.001*	
2–10 mm, mean ± SD	N/Aˆ	53.2 ± 18.0	19.8 ± 9.37	<.001*	
GDF9					
Proportion detectable, %	50 (8/16)	60 (6/10)	53 (8/15)	.883	
Baseline (early FP) pg/mL, median [95% CI] (mean ± SD)	16.0 [15.4, 23.2] (19.7 ± 6.4)	36.3 [15.4, 55.3] (392.3 ± 1140)	32.6 [15.4, 76.3] (85.2 ± 177.0)	.175	
Follicular phase, median [95% CI]	16.7 [15.4, 24.9]	35.6 [15.4, 73.9]	39.1 [15.4, 73.7]	.300	ERA vs. ARA *P*<.05
Luteal phase, median [95% CI]	15.4 [15.4, 23.6]	37.1 [15.4, 66.0]	44.8 [15.4, 95.5]	.020*	
FP vs. LP, *P* value	*P*=.160	*P*=.156	*P*=.067		
BMP15					
Proportion detectable, %	69 (11/16)	60 (6/10)	86 (12/14)	.346	
Baseline (early FP) pg/mL, median [95% CI] (mean ± SD)	48.2 [23.0, 90.9] (67.61 ± 60.5)	46.5 [23.0, 298.1] (184.3 ± 361.4)	62.1 [33.7, 127.8] (73.3 ± 43.5)	.598	
Follicular phase, median [95% CI]	49.5 [25.3, 108.8]	34.9 [23.0, 305.6]	60.5 [43.8, 114.0]	.430	
Luteal phase, median [95% CI]	56.4 [27.2, 88.7]	45.2 [23.0, 160.7]	61.7 [31.6, 93.7]	.913	
FP vs. LP, *P* value	*P*=.473	*P*=.148	*P*=.326		

Note: Age, body mass index (BMI), and proportion detectable were normally distributed and analyzed by one-way ANOVA. Cycle characteristics, antral follicle count (AFC) and GDF9/BMP15 concentration differences were analyzed by non-parametric Kruskal-Wallis tests.
ˆN/A: AFC not determined in the ERA cohort. ARA = advanced reproductive age; CI = confidence interval; ERA = early reproductive age; FP = follicular phase; IOI = interovulatory interval; LP = luteal phase; MRA = mid reproductive age; SD = standard deviation.
* Significant difference.

Riepsamen. GDF9 and BMP15 across the menstrual cycle. Fertil Steril 2021.

if they had regular menstrual cycles or <12 months of amenorrhea (i.e., had not reached menopause), as well as exhibited 2 subsequent ovulatory cycles during the study (as determined by ultrasonographic documentation of a corpus luteum and a rise in serum progesterone during the luteal phase). To approximate the minimum statistical power of this analysis, G*Power 3.1.9.2 (35) was used to perform a power calculation for a repeated measures analysis of variance (ANOVA) with 10 subjects (the smallest group in our analysis), 10 time points, and a type I error rate of 5%. This showed that the sample provides >75% power to detect an effect size of f = 0.4, which is considered a large effect by Cohen's suggested conventions (36).

Sampling Regimen

Venous blood samples were collected throughout the menstrual cycle, and serum stored frozen as described previously (6, 34).

Early reproductive age cohort (21–29 years). Serial blood samples from individual women were collected across the menstrual cycle, on days 3, 7, and 11, then daily for a maximum of 7 days or until 2 days after a positive result on daily urinary LH strip tests (Baby 4 You, Auckland, New Zealand), to capture hormone changes around the LH surge. Midluteal and late luteal samples were collected 7 and 11 days after the positive LH strip test, respectively. In the absence of a positive LH, luteal phase samples were taken on days 21 and 35 of the cycle. Urinary LH results were confirmed subsequently by quantitative serum LH immunoassays. Ovulation was defined as a peak midcycle LH surge >20 IU/L and luteal phase progesterone >15 nmol/L.

Mid reproductive age (18–35 years) and advanced reproductive age (45–50 years) cohorts. To investigate hormone dynamics across an entire cycle, blood samples were collected from individual women every Monday, Wednesday, and Friday across a complete interovulatory interval (IOI; from one ovulation to the subsequent ovulation). In addition, transvaginal ultrasound scans were performed at each visit to evaluate follicular growth of ≥2 mm (described by Vanden Brink et al. [6]). Once a dominant follicle reached ≥14 mm, scans were performed daily to determine follicle fate. Ovulation was defined as the disappearance of a dominant follicle and subsequent appearance of a corpus luteum ultrasonographically occurring in association with a rise in serum progesterone ≥15.9 nmol/L. AFC across the cycle was quantified further as described by Vanden Brink et al. (6).

GDF9 and BMP15 Assays

We previously developed and validated an enzyme-linked immunosorbent assay (ELISA) for detecting BMP15 in human serum (33) using the monoclonal antibody (mAb) 28A (37) supplied by the Oxford Brooks University (Oxford, United Kingdom) and recombinant promature human BMP15 protein supplied by Associate Professor Craig Harrison at Monash University (Clayton, Australia). As described by Riepsamen et al. (33), the BMP15 sandwich ELISA uses mAb 28A as the capture antibody and biotinylated (biot)-mAb 28A as the detection antibody, such that it detects homodimers of BMP15. Monoclonal antibody 28A is directed to an N-terminal peptide of the mature region of human BMP15 (SAEVTASSSKHSGPENNQC) (38). The BMP15 ELISA was optimized for detecting low abundance proteins in complex biological samples (33). For example, to offset assay matrix effects, an equivalent volume of non-immunoactive male serum was added to the BMP15 standard and preincubated for 1 hour before assay. Further, to counter the interference effects of heterologous antibodies present in serum, non-specific mouse IgG was added to all samples and standards during this preincubation. For the assay procedure, in brief, microtiter plates were coated with mAb 28A, washed, and stored in a blocking buffer. Preincubated standards or serum samples were added to the MAb-coated plate and incubated overnight. The plate was washed, biot-mAb was added and then incubated for 2 hours. The plate was again washed, streptavidin–horseradish peroxidase (HRP) was added and then incubated for 45 minutes. The plate was washed and a substrate for HRP (tetramethylbenzidine) was added to enable a color reaction, which was stopped with 1 M H_2SO_4, and the absorbance was read at 450 nm. A cubic spline-fitting transformation was used to fit the binding curve (39). This ELISA was used to measure serum concentrations of BMP15 in the serum samples, assayed in duplicate. The BMP15 assay sensitivity (23 pg/mL), or limit of quantification (LOQ), was defined as the dose of standard preparation corresponding to 2 times standard deviation absorbance units above the assay blank value. The intraassay variation across 7 experiments was 3.7% and interassay variation was 8.7%.

Serum concentrations of GDF9 were determined using a new commercially available ELISA for GDF9 in accordance with the manufacturer's protocol, assayed as singletons (AL-176; Lot No. 041619; Ansh Laboratory, Webster, TX, USA). This sandwich ELISA uses antibodies directed at the mature region of GDF9 and cross-reacts with promature and mature GDF9, and cumulin, the heterodimer of GDF9 and BMP15 (40). The GDF9 assay sensitivity was 15.4 pg/mL, with an intraassay variation of 2.4%. Cross-reactivity of recombinant promature human BMP15 protein (supplied by Associate Professor Craig Harrison at Monash University, Clayton, Australia) was assessed in the GDF9 ELISA. BMP15 was assayed at 12,000 pg/mL; three-fold higher than the highest dose of recombinant GDF9 calibrator. There was limited cross-reactivity (0.07%), calculated as (observed concentration/estimated concentration) x 100. Using the quality control I and II provided, the interassay variation across 9 experiments was 7.9% and 3.3%, respectively. Using an in-house quality control of pooled female serum samples, the interassay variation was 10.3%. For GDF9 and BMP15, serum samples from individual women were assayed within a plate. Samples below the LOQ were assigned the sensitivity of the assay (15.4 and 23.0 pg/mL for GDF9 and BMP15, respectively), except where concentrations were modeled using a maximum likelihood framework.

Other Reproductive Hormone Assays

Serum concentrations of other reproductive hormones were previously measured by immunoassay in all samples and assay characteristics reported (e.g., intraassay coefficients and LOQ) as described for the ERA cohort (34) and the MRA and ARA cohorts (6). In brief, FSH, LH, estradiol, and progesterone were measured by ELISA in all samples for the ERA cohort. For the MRA and ARA cohorts, FSH and LH were measured by ELISA, and estradiol and progesterone were measured by radioimmunoassay. AMH was measured in all samples from the ERA cohort (Gen II AMH, Beckman Coulter). For the MRA and ARA cohorts, an ultrasensitive pico-AMH assay was used to measure AMH in all samples, which previously has confirmed AMH values reported using the Gen II AMH, Beckman Coulter assay, but with 15-fold increased sensitivity (r = 0.9 [41]).

Statistical Analysis

Statistical analyses were performed using GraphPad Prism version 8.3.1 (39) and R version 4.0.0 (42). For the analysis of changes in GDF9 and BMP15 across the menstrual cycle, data were analyzed by 2 methods; initially for an observational comparison of binned cycle stages and subsequently using statistical modeling to account for the different sampling regimes between cohorts, different cycle lengths between women, and a large proportion of values below the LOQ. First, serum concentrations were binned into 3-day categories and analyzed as repeated measures data either by one-way ANOVA with Geisser-Greenhouse correction, or for hormones with missing data, by a mixed-effects analysis. Data that were not normally distributed were log-transformed for analysis. Second, serum concentrations were modeled to estimate changes in mean and variance across the cycle. All values were included by rescaling the data to a 28-day cycle using the observed dates of ovulation (one day after the LH surge for the ERA cohort, and using the transvaginal ultrasound observations for the MRA and ARA cohorts) and menstruation for each woman as landmark time points. Of the 16 study participants recruited in the ERA cohort, the LH assay values of 4 women displayed no surge during a limited sampling period (4–7 consecutive days from menstrual day 11); however, all women demonstrated a subsequent progesterone rise in the midluteal or late luteal phase (sampled on day 21 or 35, respectively). In these cases, the day of ovulation was estimated using the reported length of the menstrual cycle and assuming a 14-day luteal phase. Q-Q plots suggested that a log-normal distribution provided a good fit to the observed GDF9 and BMP15 concentrations, after accounting for left-censoring due to the LOQ for each assay (43). A generalized additive model for location, shape and scale (GAMLSS) (44) with adaptive cyclic penalized cubic regression splines (45) was applied to model the mean and variance of the hormone concentrations across the menstrual cycle. In addition, the model included fixed effects to account for cohort differences, random intercepts to account for differences between individuals, and a continuous autocorrelation structure (46) for the within-individual serial measurements. Serum AMH concentrations were relatively stable across the cycle, with concentrations highest in the midfollicular phase and decreasing at ovulation/immediately after the LH surge, supporting this modeling approach for analyzing dynamic hormone changes across the cycle (c.f. 8, 34, 47). We used this model to estimate the intraclass correlation coefficient (48) to assess the within-person variance for each hormone throughout the cycle as the ratio of the estimated random effect variance to the estimated total variance.

RESULTS

Participant Demographics and Cycle Characteristics

Participant demographics and menstrual cycle features were compared for the 3 cohorts of women: ERA–Otago, 21–29 years (n = 16); MRA–Saskatchewan, 18–35 years (n = 10); and ARA–Saskatchewan, 45–50 years (n = 15; Table 1). As expected, there were differences in age ($P<.0001$) and AFC ($P<.001$) between the cohorts, but no evidence of differences in BMI. The overall cycle length was significantly longer in the ERA cohort compared with the ARA ($P<.05$) cohort. Greater variability in the cycle length was detected in women of ARA compared with the younger cohorts (ERA and MRA).

Serum GDF9 and BMP15

GDF9 and BMP15 ELISAs were applied to serum samples across the menstrual cycle. Concentrations of these oocyte-secreted factors were in the pg/mL range, with 50%–86% of women having samples above the LOQ of the assays among all 3 cohorts (Table 1). There were no differences in the proportion of detectable samples among the 3 cohorts (Table 1). Baseline concentrations in the early follicular phase (menstrual days 2–4) were not significantly different between the cohorts for GDF9 or BMP15. Further, there were no differences in the mean follicular phase concentrations or luteal phase concentrations between the cohorts for BMP15. However, the luteal phase GDF9 concentrations were significantly different between cohorts ($P=.02$), with significantly higher median GDF9 in the women of the ARA cohort (45–50 years; 44.8 pg/mL; 95% CI 15.4, 95.5) than the ERA cohort (21–29 years; 15.4 pg/mL; 95% CI 15.4, 23.6; $P<.05$). Therefore, for analyses of cyclical variations, each cohort was assessed separately.

GDF9 and BMP15 Across the Menstrual Cycle

For each cohort, changes in GDF9 and BMP15 throughout the cycle were analyzed by 2 methods. First, serum concentrations were binned into 3-day categories and analyzed as repeated measures data either by one-way ANOVA or by mixed-effects analysis (for data with missing values) (Fig. 1). Second, the outcomes were centralized relative to the day of ovulation and the start of menses and normalized to a 28-day cycle, for statistical analyses appropriate for left-censored, repeated measures data (Fig. 2). A comparison of the established reproductive hormones, progesterone, estradiol, and AMH showed expected changes across the cycle, demonstrating the cyclicity of the cohorts and samples, and the

FIGURE 1

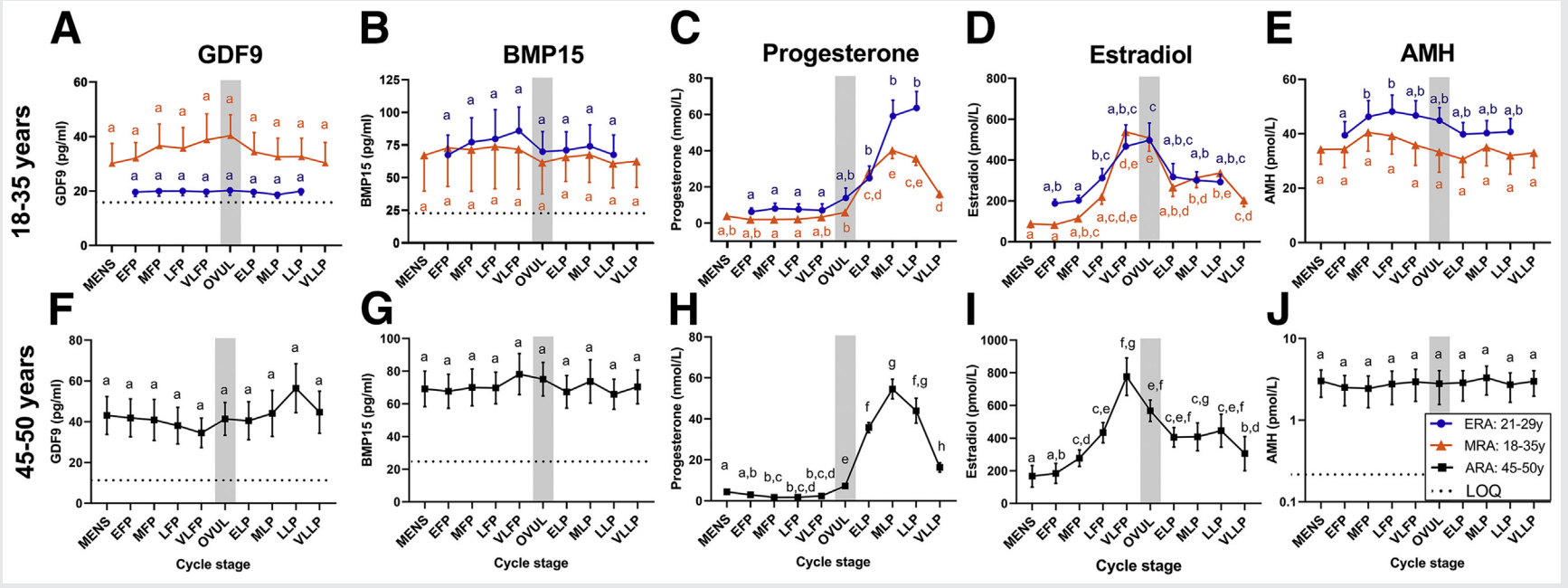

Mean serum GDF9, BMP15, progesterone, and estradiol concentrations across the menstrual cycle in women from 3 cohorts. (**A**–**E**) Early and Mid reproductive age (ERA 21–29 years (y), n = 14; Δ MRA 18–35 years, n = 8), (**F**–**H**) Advanced reproductive age (ARA 45–50 years, n = 14). Serum samples were binned into 3-day categories: menses (MENS), early follicular (EFP), midfollicular (MFP), late follicular (LFP), and very late follicular (VLFP) phases, ovulation (OVUL), early luteal (ELP), midluteal (MLP), late luteal (LLP), and very late luteal (VLLP) phases. Sera were sampled from MENS to LLP for the ERA cohort, and from ovulation to the subsequent ovulation for the MRA and ARA cohorts with groupings arranged in order of MENS to VLLP for visual comparison. Data are mean with standard error of the mean error bars, with 2 women excluded from all figures because of outlier GDF9 or BMP15 concentrations for all samples. *Gray shading* indicates ovulation. *Dashed horizontal lines* indicate the limit of quantification (LOQ). Repeated measures data were analyzed by one-way ANOVA or mixed-effects analysis (where data were missing); time points that share letters were not significantly different.

Riepsamen. GDF9 and BMP15 across the menstrual cycle. Fertil Steril 2021.

FIGURE 2

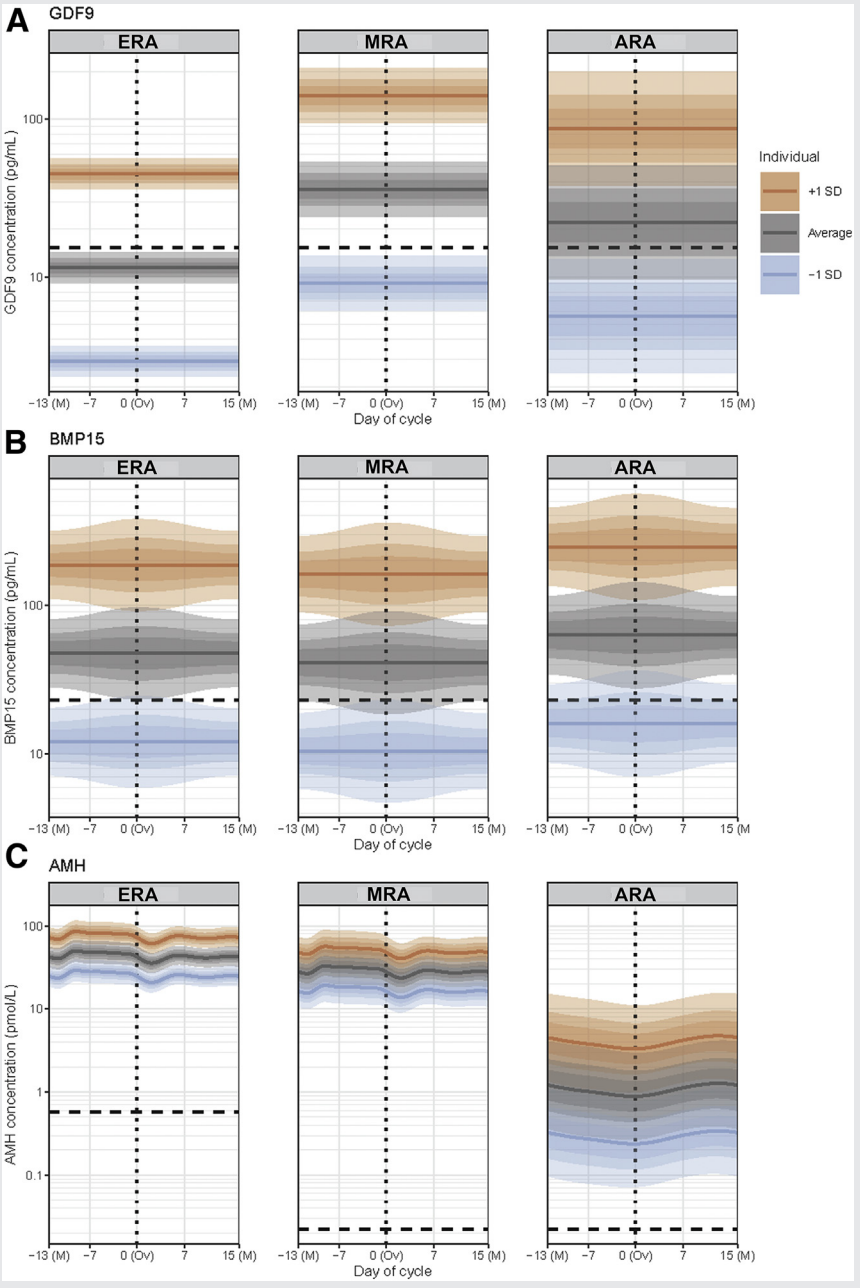

Estimated low, average, and high serum concentrations across the menstrual cycle using a generalized additive model of location, shape and scale (GAMLSS). Estimated serum GDF9 (**A**), BMP15 (**B**), and AMH (**C**) concentrations for individuals from each of the 3 cohorts: early reproductive age (ERA, 21–29 years, n = 16), mid reproductive age (MRA, 18–35 years, n = 10), and advanced reproductive age (ARA, 45–50 years, n = 15). The *gray line* represents the modeled 'average' individual for that cohort, and the *orange* and *blue lines* represent individuals whose average concentration is +1 and -1 standard deviation (SD) from the mean, respectively. *Shaded areas* indicate the within-individual variance across the cycle, showing where 50%, 75%, and 95% of the measurements would be expected. Expected concentrations were modeled using GAMLSS. Serum concentrations for each woman were constrained to be equal at the first and last days of the cycle (menses, M). Thus, where no differences were observed across the cycle, the subject response was a straight line. Due to the high between-subject variation, the change in serum patterns in individuals ±1 SD from the mean are also presented. As seen with serum BMP15 (but not GDF9), the profile exhibits high variance after midcycle, suggesting large intercycle variability compared with the beginning of the cycle. *Dotted vertical lines* indicate ovulation (Ov). *Dashed horizontal lines* indicate the limit of quantification.

Riepsamen. GDF9 and BMP15 across the menstrual cycle. Fertil Steril 2021.

FIGURE 3

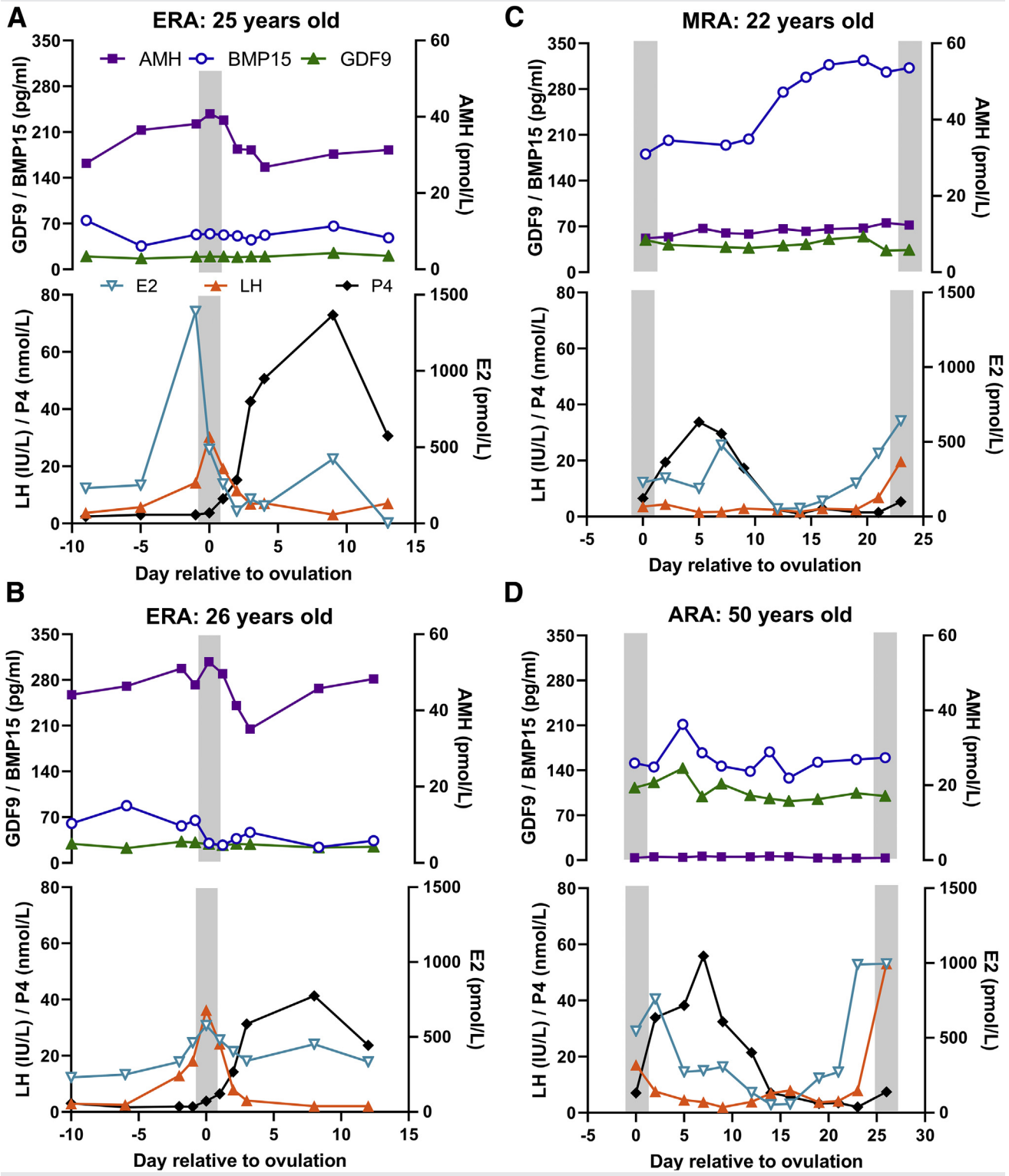

Representative individual hormone profiles for serum AMH, BMP15, GDF9, estradiol (E2), LH, and progesterone (P4) across the menstrual cycle. (**A**–**D**) Hormone profiles from 2 women from the ERA cohort from Otago (**A**) 25 and (**B**) 26 years old, and 2 from the MRA and ARA cohorts from Saskatchewan (**C**) 22 (MRA) and (**D**) 50 (ARA) years old. Limits of quantitation (LOQs) for the GDF9 and BMP15 assays were 15.4 pg/mL and 23 pg/mL, respectively. *Shaded areas* indicate ovulation (day 0).

Riepsamen. GDF9 and BMP15 across the menstrual cycle. Fertil Steril 2021.

appropriateness of the modeling methods (Fig. 1C–E and H–J, Fig. 2C).

Overall, there were no statistically significant changes in average serum GDF9 or BMP15 concentrations across the menstrual cycle in any cohort (Figs. 1 and 2). In descriptive terms, Figure 1 shows GDF9 and BMP15 highest in the mid-follicular to late follicular phases and a tendency for a decline along with the LH surge at ovulation for all cohorts (Fig. 1A, B, and G), except for women of ARA where GDF9 concentrations tended to be highest in the luteal phase (Fig. 1F) and were significantly higher than luteal phase levels in women of the ERA cohort (Table 1). Overall, these distributions across the cycle were not statistically significant when analyzed by a mixed-effects analysis of repeated measures data. A notable proportion of the samples were below the LOQ of both assays (Table 1). Therefore, a means to account for such left-censored data was applied (43), as we have done previously for serum GDF9 and BMP15 (33). This analysis revealed no changes in mean GDF9 or BMP15 across the cycle in any cohort (Fig. 2A and B). In the ERA cohort, 89 of 157 observations (57%) were below the LOQ for GDF9, and 8 of 16 individuals had >90% of their observations below the LOQ, suggesting that the average values are below the LOQ for GDF9. This resulted in the estimated mean GDF9 values below the LOQ of the GDF9 assay (Fig. 2A). Supporting the statistical modeling analyses, the expected midcycle decline in AMH was detected (Fig. 2C). There were differences in variance across the cycle for BMP15 and AMH, but not for GDF9 (Fig. 2). The variance for BMP15 was highest in the luteal phase immediately after ovulation, until 3–4 days after ovulation when variance decreased (Fig. 2b). Nonetheless, this accounted for a small proportion of the total variance, relative to the large differences between individual women and the natural within-individual variations. The intraclass correlation coefficients were high across the cycle in all cohorts, ranging from 0.91–0.99 for GDF9, 0.84–0.93 for BMP15, and 0.81–0.95 for AMH, indicating high similarity between values within a woman.

Representative serum GDF9 and BMP15 profiles during the ovarian cycle (Fig. 3) demonstrate the interindividual and intraindividual variations across the cycle, relative to LH, FSH, estradiol, progesterone, as well as AMH.

DISCUSSION

This study provides the first description of serum GDF9 and BMP15 concentrations across the menstrual cycle in healthy, ovulatory women. As oocyte products, GDF9 and BMP15 were at low circulating concentrations, with GDF9 and BMP15 detectable in only 54% and 73% of women, respectively. Suggestions of possible changes in GDF9 and BMP15 profiles across the cycle were observed; however, statistical differences were not detected with the number of observations in this study. These findings are consistent with our previous analyses showing that, in infertile women undergoing in vitro fertilization treatment, GDF9 and BMP15 serum concentrations are unchanged with exogenous FSH administration during ovarian stimulation, despite significant changes in other ovarian and pituitary reproductive hormones (33). The relative uniformity of GDF9 and BMP15 throughout the menstrual cycle may reflect that these serum concentrations are associated with the total population of oocytes within a woman's ovaries, similar to AMH. However, our previous study of 140 women found no association between serum AMH and either GDF9 or BMP15 serum concentrations (33). In humans, GDF9 is expressed abundantly in oocytes from primordial through to preovulatory follicles, and BMP15 is expressed in oocytes from secondary through to preovulatory follicles (19, 20). In contrast, changes in estrogen across the cycle are due to the production from follicles at late antral stages of development only, and progesterone is a reflection of luteal growth, which occurs after the ovulation of late antral stage follicles. Thus, serum GDF9 and BMP15 concentrations do not appear to reflect the oocytes of FSH-dependent follicles recruited during the follicular phase, despite BMP15 being known to regulate granulosa cell sensitivity to FSH (49).

GDF9 and BMP15 are principally regarded as oocyte-secreted growth factors (20), and therefore, may be expected to decline in women of ARA compared with the younger cohorts. However, we did not observe this, in fact, luteal phase GDF9 concentrations were significantly higher in the women of ARA compared with the ERA cohort. Although unexpected, these findings are consistent with our previous analyses showing that GDF9 and BMP15 do not decline appreciably with age in women of reproductive age and that GDF9 (but not BMP15) persists in postmenopausal serum (33). These findings are notable in that the current study and the previous study by Riepsamen et al. (33) were conducted using different GDF9 assays, but the same BMP15 assay. The current study used a newly available GDF9 ELISA (Ansh Labs), whereas previously, we used an in-house developed ELISA (33). The 2 GDF9 assays use differing monoclonal antibody pairs, each directed at differing portions of the mature domain of GDF9. Despite these assay differences, both assays have detected GDF9 in the serum of perimenopausal women, which is an unexpected finding given the low number of oocytes remaining in these women, suggesting that the GDF9 detected in these women is likely to be of non-oocyte origin. Extensive databases of high-throughput gene expression studies of normal human tissues (50) allow comparison of the expression profiles of GDF9 and BMP15 in various human tissues. This shows that GDF9 and BMP15 mRNA are massively enriched in the ovaries and testes compared with other tissue types. Nonetheless, mRNA expression has been reported in the pituitary, testis, and other tissues of some species, indicating that these factors do not have actions exclusive to the ovary (9, 49, 51–53).

A small decline in BMP15 may be apparent along with the midcycle LH surge. In addition, increased variance in BMP15 was detected in the early luteal phase for all cohorts. Oocyte-secreted GDF9 and BMP15 have well-characterized roles in the regulation of ovulatory events, including enabling the LH-induced EGF-like peptide cascade and cumulus cell mucification, as well as the terminal granulosa/cumulus cell differentiation (28, 29). In rodents, ovulation leads to rapid export of promature and mature BMP15 proteins from the oocyte into the extracellular space of the follicle and a concomitant decline in oocyte expression of Bmp15 and

Gdf9 mRNA (30–32). Regulation of BMP15 in the mouse is known to be different from that of monovular species. Nonetheless, these studies showed that there is evidence of periovulatory regulation in BMP15, which may account for the possible decrease in serum BMP15 over the periovulatory period in the current study. The serum BMP15 profile appears similar to AMH, with a decline observed around the time of ovulation. Nonetheless, the serum concentrations measured here may reflect only part of the physiology of GDF9 and BMP15 within the ovary, because it is unknown at this stage if the molecular forms of GDF9 and BMP15 present in serum and detected by the ELISAs represent the bioactive forms acting as paracrine factors within the follicle.

A limitation of this study was the large proportion of samples below the limit of detection for the GDF9 and BMP15 assays, despite the assay sensitivities being in the pg/mL range. Further, this study combined 3 cohorts from 2 independent previously published studies with different sampling regimes. Therefore, it was necessary to apply statistical modeling that could account for such observations. In this study, the statistical models for GDF9 and BMP15 were similar to those suggested by Zhang et al. (54, 55) and Roy et al. (56) for cyclical hormones (e.g., spline regression and mixed models), but fit using maximum penalized likelihood under the GAMLSS framework. This provided the ability to handle observations below the LOQ, and to incorporate adaptive smoothness that allows for the modeling of, for example, either slow or fast changes in the response variable over time (45). Other approaches for cyclical hormone modeling, such as functional data analysis (57), could be adapted to be used for a similar analysis. Another limitation is that the number of individuals in each cohort was small. However, the large number of repeated measurements from each subject ensured that there was sufficient power to detect medium-to-large changes in hormone concentrations over time. An assessment of small-to-medium changes across the cycle and their biological relevance and assessment of the high variance in BMP15 around ovulation would require more frequent sampling in a large population of women, as shown for AMH (8). However, in a clinical setting, it is unknown whether such minor changes in GDF9 and BMP15 would be consequential, as seen with AMH where measurement is done irrespective of the day of the menstrual cycle, despite small changes across the cycle (58).

CONCLUSION

GDF9 and BMP15 are the first oocyte-secreted biomarkers with the potential clinical application as markers of oocyte quality and quantity. However, no studies have been conducted to assess if they are altered across the menstrual cycle, and if the assessment should be confined to specific stages of the cycle. Our preliminary analyses show that serum concentrations of GDF9 and BMP15 vary significantly between women, but may be relatively unchanged across the menstrual cycle in women of reproductive age and ARA. Further research efforts in this area using more sensitive assays can be expected to reveal whether these essential oocyte-secreted growth factors prove useful diagnostic biomarkers of female fecundity, ovarian dysfunction, and/or oocyte quality.

Acknowledgments: The investigators are grateful for assistance from Prof. Craig Harrison, Dr. Kelly Walton and Dr. William Stocker of Monash University, Australia for providing recombinant proteins, to Oxford Brookes University, United Kingdom for provision of the monoclonal antibodies, and to Ansh Labs for access to GDF9 ELISAs. Thanks are also extended to Ms. Heidi Vanden Brink M.Sc. for assistance with data collection at the University of Saskatchewan. The work was funded by a grant (APP1121504) awarded to R.B.G., D.M.R., and W.L.L. and fellowships (APP1023210, APP1117538) awarded to R.B.G. from the National Health and Medical Research Council of Australia, and by funds from City Fertility Centre Global Pty. Ltd.

REFERENCES

1. Barbieri RL. The endocrinology of the menstrual cycle. Methods Mol Biol 2014;1154:145–69.
2. Broekmans FJ, Soules MR, Fauser BC. Ovarian aging: mechanisms and clinical consequences. Endocr Rev 2009;30:465–93.
3. Hale GE, Zhao X, Hughes CL, Burger HG, Robertson DM, Fraser IS. Endocrine features of menstrual cycles in middle and late reproductive age and the menopausal transition classified according to the Staging of Reproductive Aging Workshop (STRAW) staging system. J Clin Endocrinol Metab 2007; 92:3060–7.
4. Landgren BM, Collins A, Csemiczky G, Burger HG, Baksheev L, Robertson DM. Menopause transition: annual changes in serum hormonal patterns over the menstrual cycle in women during a nine-year period prior to menopause. J Clin Endocrinol Metab 2004;89:2763–9.
5. Robertson DM, Lee CH, Baerwald A. Interrelationships among reproductive hormones and antral follicle count in human menstrual cycles. Endocr Connect 2016;5:98–107.
6. Vanden Brink H, Robertson DM, Lim H, Lee C, Chizen D, Harris G, et al. Associations between antral ovarian follicle dynamics and hormone production throughout the menstrual cycle as women age. J Clin Endocrinol Metab 2015;100:4553–62.
7. van Disseldorp J, Faddy MJ, Themmen AP, de Jong FH, Peeters PH, van der Schouw YT, et al. Relationship of serum antimullerian hormone concentration to age at menopause. J Clin Endocrinol Metab 2008;93: 2129–34.
8. Kissell KA, Danaher MR, Schisterman EF, Wactawski-Wende J, Ahrens KA, Schliep K, et al. Biological variability in serum anti-Mullerian hormone throughout the menstrual cycle in ovulatory and sporadic anovulatory cycles in eumenorrheic women. Hum Reprod 2014;29:1764–72.
9. Aaltonen J, Laitinen MP, Vuojolainen K, Jaatinen R, Horelli-Kuitunen N, Seppä L, et al. Human growth differentiation factor 9 (GDF-9) and its novel homolog GDF-9B are expressed in oocytes during early folliculogenesis. J Clin Endocrinol Metab 1999;84:2744–50.
10. Dalbies-Tran R, Cadoret V, Desmarchais A, Elis S, Maillard V, Monget P, et al. A comparative analysis of oocyte development in mammals. Cells 2020;9: 1002.
11. Dong J, Albertini DF, Nishimori K, Kumar TR, Lu N, Matzuk MM. Growth differentiation factor-9 is required during early ovarian folliculogenesis. Nature 1996;383:531–5.
12. Gilchrist RB, Lane M, Thompson JG. Oocyte-secreted factors: regulators of cumulus cell function and oocyte quality. Hum Reprod Update 2008;14: 159–77.
13. Persani L, Rossetti R, Di Pasquale E, Cacciatore C, Fabre S. The fundamental role of bone morphogenetic protein 15 in ovarian function and its involvement in female fertility disorders. Hum Reprod Update 2014;20:869–83.
14. Sánchez F, Smitz J. Molecular control of oogenesis. Biochim Biophys Acta Mol Basis Dis 2012;1822:1896–912.

15. Heath DA, Pitman JL, McNatty KP. Molecular forms of ruminant BMP15 and GDF9 and putative interactions with receptors. Reproduction 2017;154: 521–34.
16. Mottershead DG, Sugimura S, Al-Musawi SL, Li JJ, Richani D, White MA, et al. Cumulin, an oocyte-secreted heterodimer of the transforming growth factor-β family, is a potent activator of granulosa cells and improves oocyte quality. J Biol Chem 2015;290:24007–20.
17. Grøndahl ML, Borup R, Vikeså J, Ernst E, Andersen CY, Lykke-Hartmann K. The dormant and the fully competent oocyte: comparing the transcriptome of human oocytes from primordial follicles and in metaphase II. Mol Hum Reprod 2013;19:600–17.
18. Kristensen SG, Andersen K, Clement CA, Franks S, Hardy K, Andersen CY. Expression of TGF-beta superfamily growth factors, their receptors, the associated SMADs and antagonists in five isolated size-matched populations of preantral follicles from normal human ovaries. Mol Hum Reprod 2014;20:293–308.
19. Zhang Y, Yan Z, Qin Q, Nisenblat V, Chang H-M, Yu Y, et al. Transcriptome landscape of human folliculogenesis reveals oocyte and granulosa cell interactions. Mol Cell 2018;72:1021–34.e4.
20. Juengel JL, McNatty KP. The role of proteins of the transforming growthfactor-beta superfamily in the intraovarian regulation of follicular development. Hum Reprod Update 2005;11.
21. Kristensen SG, Andersen K, Møllgård K, Andersen CY. Expression of TGF-β superfamily growth factors and their receptors, the associated SMADs, and antagonists in five isolated size-matched populations of human preantral follicles from normal ovaries. Biol Reprod 2012;87:72.
22. Kristensen SG, Kumar A, Kalra B, Pors SE, Bøtkjær JA, Mamsen LS, et al. Quantitative differences in TGF-β family members measured in small antral follicle fluids from women with or without PCO. J Clin Endocrinol Metab 2019;104:6371–84.
23. Scaramuzzi RJ, Baird DT, Campbell BK, Driancourt M-A, Dupont J, Fortune JE, et al. Regulation of folliculogenesis and the determination of ovulation rate in ruminants. Reprod Fertil Dev 2011;23:444–67.
24. Patiño LC, Walton KL, Mueller TD, Johnson KE, Stocker W, Richani D, et al. BMP15 mutations associated with primary ovarian insufficiency reduce expression, activity, or synergy with GDF9. J Clin Endocrinol Metab 2017; 102:1009–19.
25. Rossetti R, Ferrari I, Bestetti I, Moleri S, Brancati F, Petrone L, et al. Fundamental role of BMP15 in human ovarian folliculogenesis revealed by null and missense mutations associated with primary ovarian insufficiency. Hum Mutat 2020;41:983–97.
26. Rossetti R, Ferrari I, Bonomi M, Persani L. Genetics of primary ovarian insufficiency. Clin Genet 2017;91:183–98.
27. Simpson CM, Robertson DM, Al-Musawi SL, Heath DA, McNatty KP, Ritter LJ, et al. Aberrant GDF9 expression and activation are associated with common human ovarian disorders. J Clin Endocrinol Metab 2014;99:E615–24.
28. Richani D, Gilchrist RB. The epidermal growth factor network: role in oocyte growth, maturation and developmental competence. Hum Reprod Update 2018;24:1–14.
29. Russell DL, Gilchrist RB, Brown HM, Thompson JG. Bidirectional communication between cumulus cells and the oocyte: old hands and new players? Theriogenology 2016;86:62–8.
30. Guéripel X, Brun V, Gougeon A. Oocyte bone morphogenetic protein 15, but not growth differentiation factor 9, is increased during gonadotropin-induced follicular development in the immature mouse and is associated with cumulus oophorus expansion. Biol Reprod 2006;75:836–43.
31. Mester B, Ritter LJ, Pitman JL, Bibby AH, Gilchrist RB, McNatty KP, et al. Oocyte expression, secretion and somatic cell interaction of mouse bone morphogenetic protein 15 during the peri-ovulatory period. Reprod Fertil Dev 2015;27:801–11.
32. Yoshino O, McMahon HE, Sharma S, Shimasaki S. A unique preovulatory expression pattern plays a key role in the physiological functions of BMP-15 in the mouse. Proc Natl Acad Sci U S A 2006;103:10678–83.
33. Riepsamen AH, Chan K, Lien S, Sweeten P, Donoghoe MW, Walker G, et al. Serum concentrations of oocyte-secreted factors BMP15 and GDF9 during IVF and in women with reproductive pathologies. Endocrinology 2019; 160:2298–313.
34. Pankhurst MW, Chong YH. Variation in circulating antimullerian hormone precursor during the periovulatory and acute postovulatory phases of the human ovarian cycle. Fertil Steril 2016;106:1238–43.e2.
35. Faul F, Erdfelder E, Lang A-G, Buchner A. G*Power 3: A flexible statistical power analysis program for the social, behavioral, and biomedical sciences. Behav Res Methods 2007;39:175–91.
36. Cohen J. Statistical power analysis for the behavioral sciences. 2nd ed. Oxfordshire, United Kingdom: Routledge; 1988.
37. RRID:AB_2801395. BMP-15/GDF-9B Antibody (28A). Available at: https://scicrunchorg/resolver/AB_2801395. Accessed October 1, 2019.
38. Pulkki MM, Myllymaa S, Pasternack A, Lun S, Ludlow H, Al-Qahtani A, et al. The bioactivity of human bone morphogenetic protein-15 is sensitive to C-terminal modification: characterization of the purified untagged processed mature region. Mol Cell Endocrinol 2011;332:106–15.
39. GraphPad Prism version 8.3.1 for Windows. GraphPad Software, La Jolla, CA, USA.
40. Kalra B, Chowdavarapu K, Patel A, Mistry S, Budhavarapu V, Savjani G, et al. Development of novel elisas for human GDF9 and BMP15 homodimers and the GDF9: BMP15 heterodimer. In: 99th Annual Meeting of the Endocrine Society. Endocrine Society; 2017.
41. Robertson DM, Kumar A, Kalra B, Shah S, Pruysers E, Vanden Brink H, et al. Detection of serum antimullerian hormone in women approaching menopause using sensitive antimüllerian hormone enzyme-linked immunosorbent assays. Menopause 2014;21:1277–86.
42. R Core Team. R: A language and environment for statistical computing. R Foundation for Statistical Computing, Vienna, Austria. Available at: http://www.R-project.org/. Accessed September 20, 2020.
43. Waller LA, Turnbull BW. Probability plotting with censored data. Am Statistician 1992;46:5–12.
44. Rigby RA, Stasinopoulos DM. Generalized additive models for location, scale and shape. J R Stat Soc Ser C Appl Stat 2005;54:507–54.
45. Wood SN. Generalized additive models: an introduction with R. 2nd ed. Boca Raton, FL: Chapman and Hall/CRC Press; 2017.
46. Pinheiro JC, Bates DM. Mixed-effects models in S and S-PLUS. New York, NY: Springer; 2000.
47. Ledger WL. Clinical utility of measurement of anti-Mullerian hormone in reproductive endocrinology. J Clin Endocrinol Metab 2010;95:5144–54.
48. McGraw KO, Wong SP. Forming inferences about some intraclass correlation coefficients. Psychol Methods 1996;1:30–46.
49. Otsuka F, Shimasaki S. A novel function of bone morphogenetic protein-15 in the pituitary: selective synthesis and secretion of FSH by gonadotropes. Endocrinology 2002;143:4938–41.
50. Suntsova M, Gaifullin N, Allina D, Reshetun A, Li X, Mendeleeva L, et al. Atlas of RNA sequencing profiles for normal human tissues. Sci Data 2019;6:36.
51. Fitzpatrick SL, Sindoni DM, Shughrue PJ, Lane MV, Merchenthaler IJ, Frail DE. Expression of growth differentiation factor-9 messenger ribonucleic acid in ovarian and nonovarian rodent and human tissues. Endocrinology 1998;139:2571–8.
52. Galloway SM, McNatty KP, Cambridge LM, Laitinen MP, Juengel JL, Jokiranta TS, et al. Mutations in an oocyte-derived growth factor gene (BMP15) cause increased ovulation rate and infertility in a dosage-sensitive manner. Nat Genet 2000;25:279–83.
53. Wang Y, Nicholls PK, Stanton PG, Harrison CA, Sarraj M, Gilchrist RB, et al. Extra-ovarian expression and activity of growth differentiation factor 9. J Endocrinol 2009;202:419–30.
54. Zhang D, Lin X, Raz J, Sowers M. Semiparametric stochastic mixed models for longitudinal data. J Am Stat Assoc 1998;93:710–9.
55. Zhang D, Lin X, Sowers M. Semiparametric regression for periodic longitudinal hormone data from multiple menstrual cycles. Biometrics 2000;56:31–9.
56. Roy A, Danaher M, Mumford SL, Chen Z. A Bayesian order-restricted model for hormonal dynamics during menstrual cycles of healthy women. Stat Med 2012;31:2428–40.
57. Meyer PM, Zeger SL, Harlow SD, Sowers M, Crawford S, Luborsky JL, et al. Characterizing daily urinary hormone profiles for women at midlife using functional data analysis. Am J Epidemiol 2007;165:936–45.
58. La Marca A, Stabile G, Artenisio AC, Volpe A. Serum anti-Mullerian hormone throughout the human menstrual cycle. Hum Reprod 2006;21:3103–7.